Plateforme de l'ICMMO

Service Magnétométrie

UNIVERSITÉ PARIS SUD

Comprendre le monde, construire l'avenir®

- MPMS 5 (1996) :

  - dc measurements,
  - 2-400K, (temperature sweep mode from 5 to 400K
  - +/- 5T

- XL7 (2012) :
  - 2-400K, up to 7T, dc measurement,
  - dc measurements, RSO,
  - ac measurements (0.1-1500Hz),
  - oven option: up to 800K (SP2M team)
- He reliquifier (Cryomech PT410)

Photomagnetic measurements:

UV/Vis or Vis/IR Fiberoptic Sample Holder

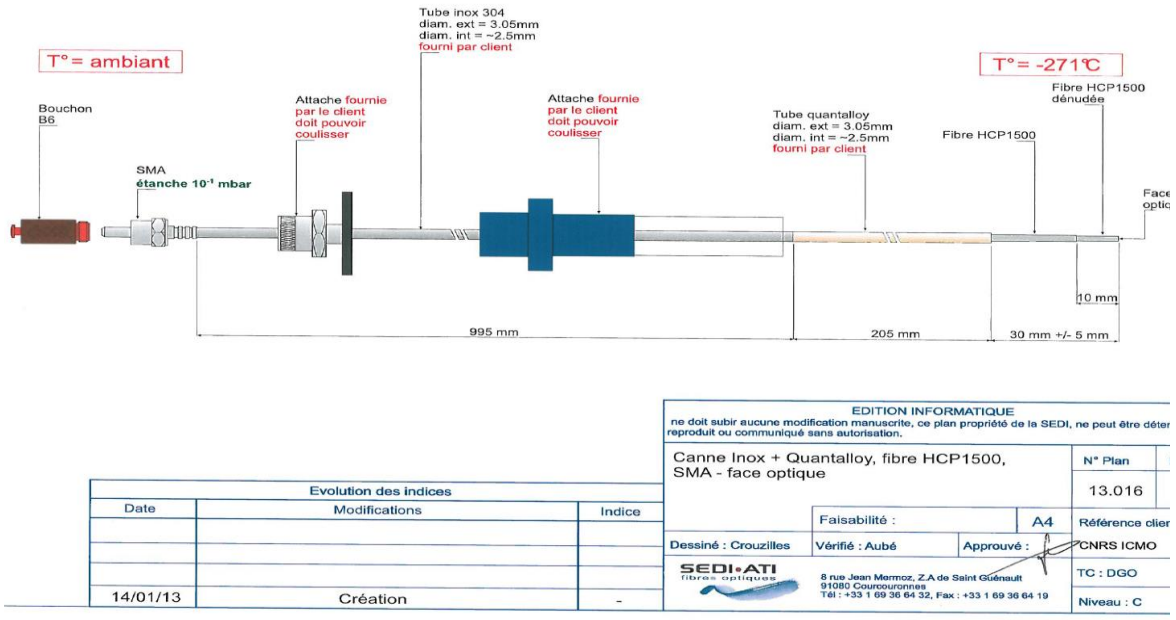

Lightning sources:

Pulsed Laser
Surelite Continuum
355nm +
OPO (410-1600 nm)

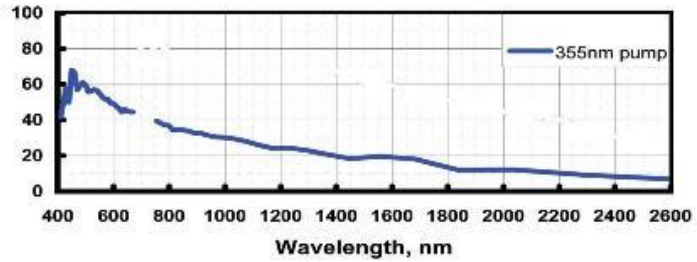

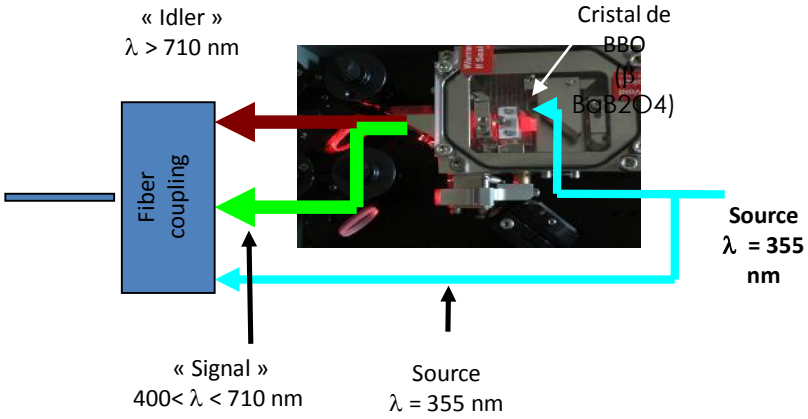

Continuous Wave Sources:

- Laser Diode (100mW max) : 405, 473, 532, 635 nm
  Low-power diode (5 mW) : 1290-1330 nm

- LED (50 mW max) : 365, 375, 385, 505, 590, 850 nm

Area of competence :

- Molecular Complexes

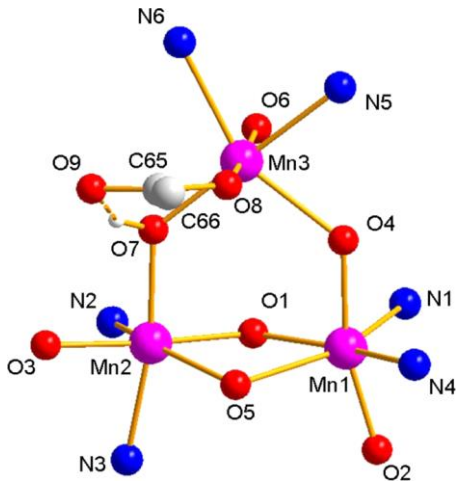

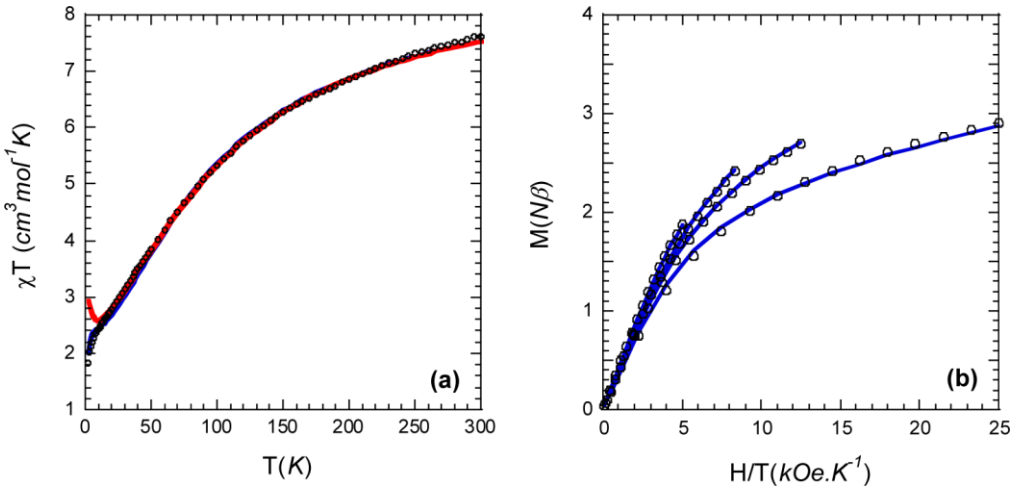

(a) Temperature dependence of $\chi_M T$ for compound $1ClO_4$: (O) experimental data, solid line in red shows the simulation obtained with the isotropic Hamiltonian (fitting in the range 300−50 K), solid line in blue corresponds to the best fit including a local zero-field splitting parameter D (fitting in the range 300−2 K). (b) Magnetization vs H/T curves recorded at 2, 4, 6, and 10 K. Solid lines correspond to the curves determined using the parameters deduced from the $\chi_M T = f(T)$ curve.

Complexes moléculairesTrinuclear Manganese Complexes of Unsymmetrical Polypodal Diamino N3O3 Ligands with an Unusual [Mn3(μ-OR)4]5+ Triangular Core: Synthesis, Characterization, and Catalase Activity, *Inorg. Chem*. **2014**, 53, 2545−2553

Area of competence :

- Single Molecule Magnet

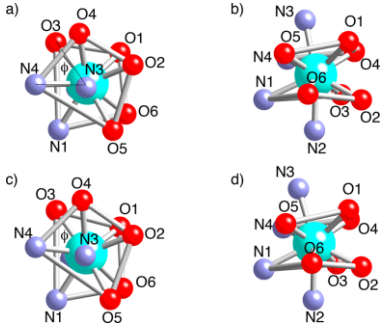

Perspective showing the distorted bicapped square-antiprismatic geometries of the central dysprosium(III) ion for 1 (a and b) and 2 (c and d).

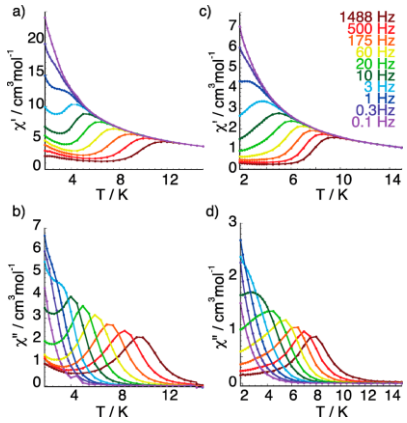

ac susceptibility data for complexes 1 (a and b) and 2 (c and d). Plots of χ′ (a and c) and χ″ (b and d) versus temperature at different wave frequencies under a dc field (H = 1000 Oe).

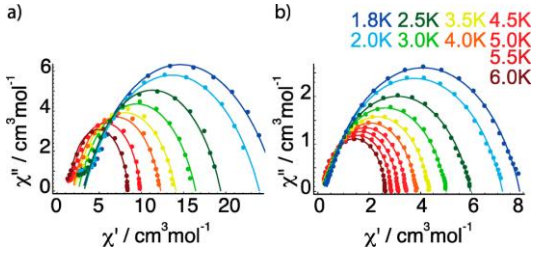

Cole−Cole plots obtained for complexes 1 (a) and 2 (b). The solid lines represent the fit obtained with a generalized Debye model.

Structural and Electronic Dependence of the Single-Molecule-Magnet Behavior of Dysprosium(III) Complexes, *Inorg. Chem*. **2014**, 53, 2598−2605

Area of competence :

- Nanoparticules

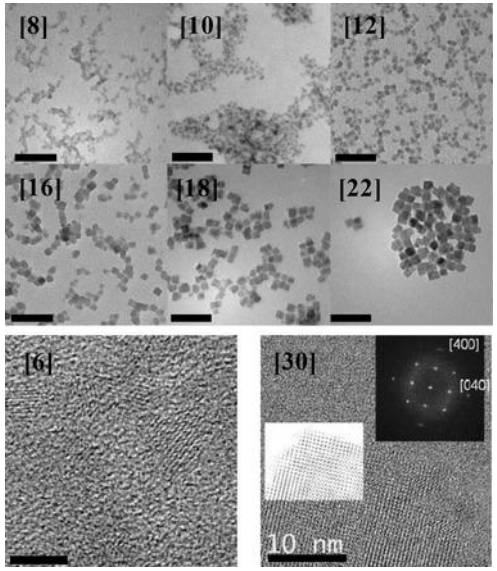

TEM images of the nanoparticles [8], [10], [12], [16], [18] and [22] embedded in DODA+ (top, scale bar: 100 nm) and HRTEM images of the nanoparticles [6] (bottom left, scale bar: 5 nm) and [30] (bottom right, insert: electronic diffraction pattern).

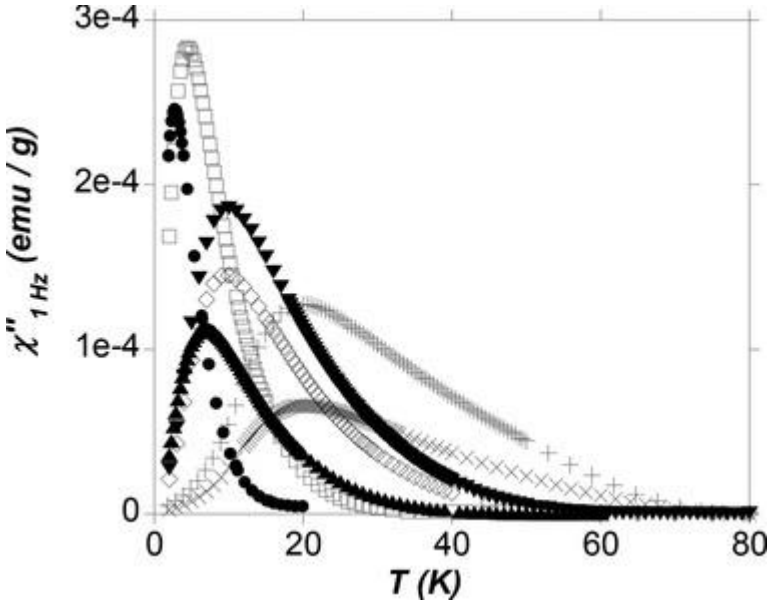

Out-of-phase component, χ″, of the magnetic susceptibility at 1 Hz for the highly diluted samples [6_dil] (●), [8_dil] (□), [10_dil] (▲), [12_dil] (◇), [16_dil] (▼), [18_dil] (+) and [22_dil] (×).

Magnetization Reversal in $CsNi^{II}Cr^{III}(CN)_6$ Coordination Nanoparticles: Unravelling Surface Anisotropy and Dipolar Interaction Effects, *Adv. Funct. Mater*. **2014**, 24, 5402–5411

Area of competence :

- Spin Convertion / LIESST effect

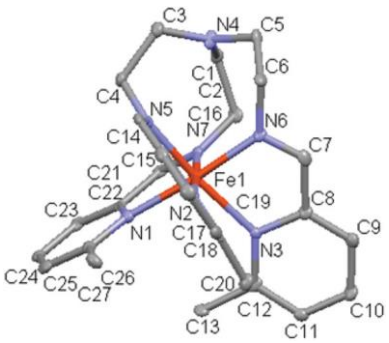

Molecular structure of the $[Fe(mepy)_3tren]^{2+}$ cation at 10 K

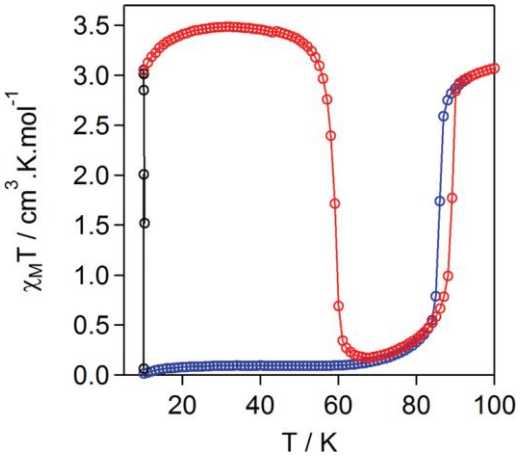

Magnetic measurement of the $Fe(mepy)_3tren](PF_6)_2 \cdot C_7H_8 \cdot C_2H_3N$ sample performed with a sweeping rate at 0.3 K min^{-1}: on cooling (blue), upon irradiation at 10 K with λ = 532 nm (black) and upon heating in the dark after reaching the photostationary state at 10 K.

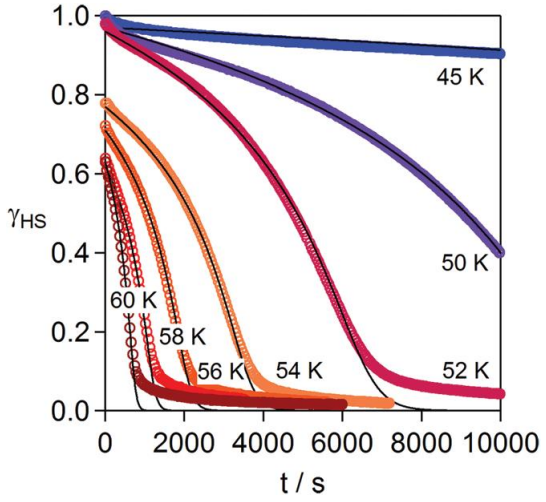

HS-to-LS relaxation curves performed with magnetization measurements at different temperatures (○), along with their modelization in the mean-field approximation (-).

Light-induced excited spin state trapping effect on $[Fe(mepy)_3tren](PF_6)_2$ solvated crystals. *Dalton Trans*., **2014**, 43, 1063–1071

Area of competence :

- LIESST Effect (2)

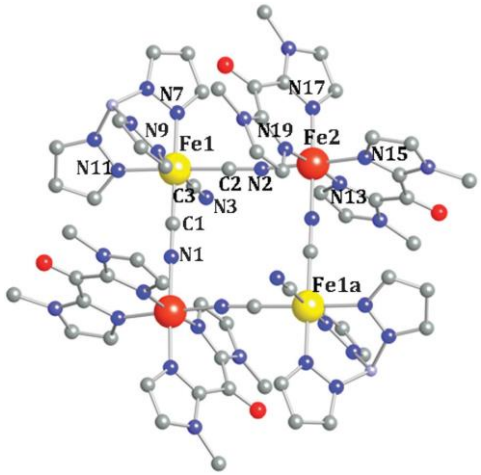

View of the cyanide-bridged $\{Fe^{III}_2Fe^{II}_2\}$ square unit with the atom labelling for the metal environments. The hydrogen atoms are omitted for clarity. C: gray, N: blue, O: red, B: pale blue, Fe^{III}: yellow, Fe^{II}: orange

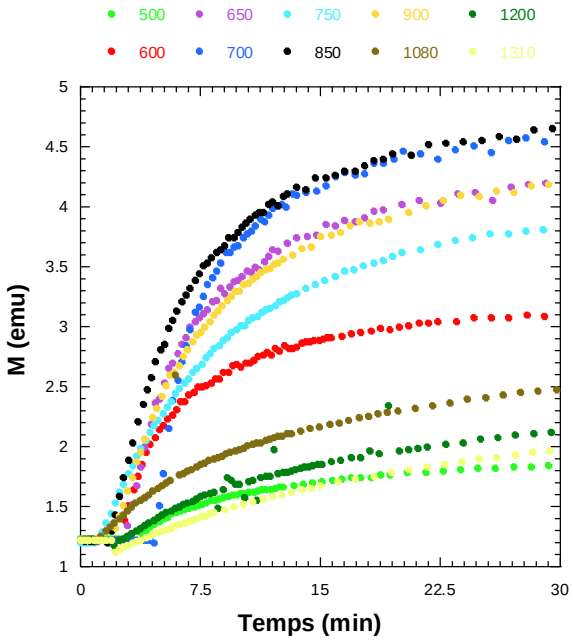

Magnetization *vs.* irradiation time of a dehydrated sample of **1** at different Wavelengths (7 mW/cm2).

Photomagnetic effect in a cyanide-bridged mixed-valence $\{Fe^{II}_2Fe^{III}_2\}$ molecular square, *Chem. Commun.*, **2012**, 48, 5653–5655

Area of competence :

- Molecular-scale devices

CoFe PBAs of chemical formula $C_xCo_4[Fe(CN)_6]_{(8+x)/3}\cdot H_2O$ (C is an alkali cation) is well tuned, they are composed of Co^{III}(low spin, LS) and Fe^{II}(LS) diamagnetic ions at low temperature. Irradiation in the visible range induces the $Co^{III}(LS)Fe^{II}(LS) \rightarrow Co^{II}$(high spin, HS)$Fe^{III}$(LS) electron transfer.

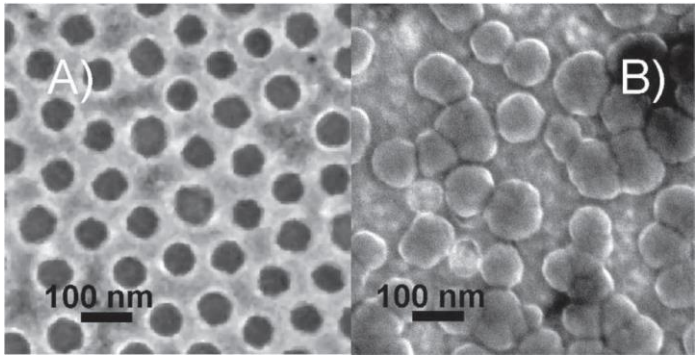

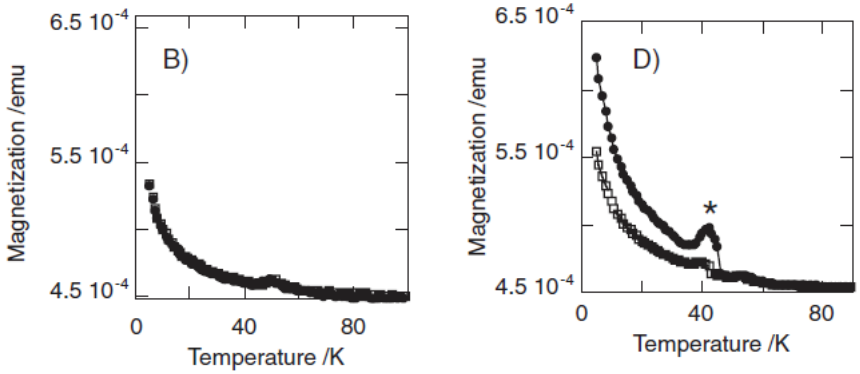

Temperature dependence of the magnetization under an applied field of 30 000 Oe of B) the PBA-free nanoperforated titanium oxide film coated on a gold layer and D) the nanocomposite coated on a gold layer before irradiation (white square) and after irradiation (black circle). A NiO antiferromagnetic thin pellet was added to the films in order to optimize the signal to noise ratio.

Tailor-made Nanometer-scale Patterns of Photo-switchable Prussian Blue Analogues, *Adv. Mater.* **2010**, *22*, 3992–3996

Area of competence :

- Measurement of molecular networks on surfaces

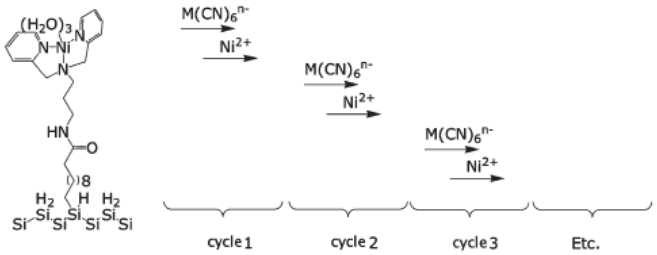

Growth of NiCr films on Ni0 anchoring sites. SGS were performed on the Ni0 anchoring sites that form a relatively flat monolayer on a Si(100) substrate. We carried out SGS by immersing alternatively the functionalized substrate in an aqueous solution of $[Cr(CN)_6]^{3-}$ (steps Cr1, Cr2,…Crn) and in a methanolic solution of $Ni(H_2O)_6^{2+}$

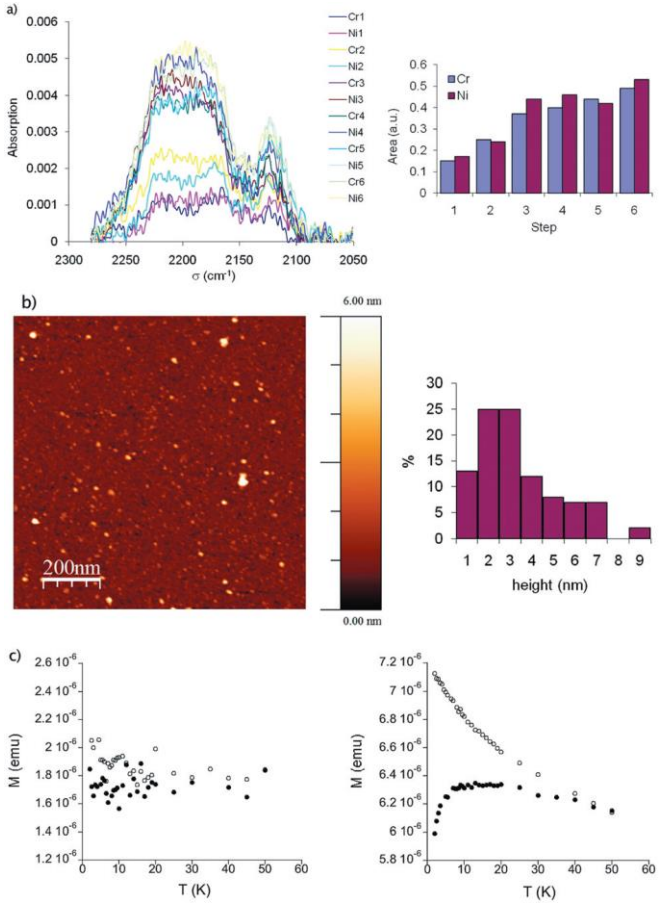

NiCr SGS (6 cycles): a) Evolution of the intensity of the infrared asymmetric vibration band of cyanide at each step from the step Ni1 to Ni6 and corresponding peak area. b) AFM image and size distributions of the objects at the step Ni6. c) M = f(T) curves at H = 100 Oe for a bare silicon wafer (left) and at the step Ni6 of NiCr SGS (right) – plain circles: ZFC, open circles: FC.

Cyanide-bridged NiCr and alternate NiFe–NiCr magnetic ultrathin films on functionalized Si(100) surface, *Dalton Trans*., **2012,** 41, 4445–4450